Colloquia: FATA 2019

# Performance of the ToF detectors in the FOOT experiment

G. Traini[12][21], A. Alexandrov[10][19][33][34], B. Alpat[11], G. Ambrosi[11],
S. Argiró[28][17], D. R. Arteche[30], N. Bartosik[17], G. Battistoni[8],
N. Belcari[3][2], E. Bellinzona[15], S. Biondi[5][20], M. G. Bisogni[3][2],
G. Bruni[5], N. Camarlinghi[3][2], P. Carra[3][2], P. Cerello[17],
E. Ciarrocchi[3][2], A. Clozza[7], S. Colombi[15][16], G. De Lellis[10][19],
A. Del Guerra[3][2], M. De Simoni[26][12], A. Di Crescenzo[10][19],
M. Donetti[17][1], Y. Dong[8][23], M. Durante[6][32], M. Emde[4],
R. Faccini[26][12], V. Ferrero[17][28], F. Ferroni[12][26], E. Fiandrini[11][24],
C. Finck[14], E. Fiorina[15][1], M. Fischetti[22][12], M. Francesconi[3][2],
M. Franchini[5][20], G. Franciosini[26][12], G. Galati[10], L. Galli[2],
V. Gentile[31], G. Giraudo[17], R. Hetzel[4], E. Iarocci[7], M. Ionica[11],
K. Kanxheri[11], A. C. Kraan[2], V. Lante[1], A. Lauria[10][19],
C. La Tessa[15][16], E. Lopez Torres[30][17], C. Massimi[20], I. Mattei[8],
M. Marafini[22][14], A. Mengarelli[5], R. Mirabelli[26][12][21],
M. C. Montesi[10][19], M. C. Morone[13][27], M. Morrocchi[2][3],
A. Moggi[2], S. Muraro[8], L. Narici[13][27], A. Pastore[29], N. Pastrone[17],
V. Patera[22][12][21], F. Pennazio[17], P. Placidi[11][25], M. Pullia[1],
F. Raffaelli[2], L. Ramello[18][17], R. Ridolfi[20], V. Rosso[3][2],
M. Rovituso[15], C. Sanelli[7], A. Sarti[22][12][21], G. Sartorelli[5][20],
O. Sato[9], L. Scavarda[28][17], A. Savazzi[1], A. Schiavi[22][12],
C. Schuy[6], E. Scifoni[15], A. Sciubba[22][12][21], M. Selvi[5], L. Servoli[11],
A. Sécher[14], G. Silvestre[11][24], M. Sitta[18][17], R. Spighi[5], E. Spiriti[7],
G. Sportelli[3][2], A. Stahl[4], S. Tomassini[7], F. Tommasino[15][16],
T. Valeri[10], S. M. Valle[8], M. Vanstalle[14], M. Villa[5][20], U. Weber[6]
and A. Zoccoli[5][20]

([1]) *Centro Nazionale di Adroterapia Oncologica (CNAO) - Pavia, Italy*
([2]) *Istituto Nazionale di Fisica Nucleare (INFN), Sezione di Pisa - Pisa, Italy*
([3]) *University of Pisa, Department of Physics - Pisa, Italy*
([4]) *RWTH Aachen University, Physics Institute III B - Aachen, Germany*
([5]) *Istituto Nazionale di Fisica Nucleare (INFN), Sezione di Bologna - Bologna, Italy*
([6]) *Biophysics Department, GSI Helmholtzzentrum für Schwerionenforschung - Darmstadt, Germany*
([7]) *Istituto Nazionale di Fisica Nucleare (INFN), Laboratori Nazionali di Frascati - Frascati, Italy*
([8]) *Istituto Nazionale di Fisica Nucleare (INFN), Sezione di Milano - Milano, Italy*
([9]) *Nagoya University, Department of Physics - Nagoya, Japan*
([10]) *Istituto Nazionale di Fisica Nucleare (INFN), Sezione di Napoli - Napoli, Italy*
([11]) *Istituto Nazionale di Fisica Nucleare (INFN), Sezione di Perugia - Perugia, Italy*
([12]) *Istituto Nazionale di Fisica Nucleare (INFN), Sezione di Roma 1 - Rome, Italy*
([13]) *University of Rome Tor Vergata, Department of Physics - Rome, Italy*
([14]) *Université de Strasbourg, CNRS, IPHC UMR 7871 - F-67000 Strasbourg, France*
([15]) *Trento Institute for Fundamental Physics and Applications, Istituto Nazionale di Fisica Nucleare (TIFPA-INFN) - Trento, Italy*
([16]) *University of Trento, Department of Physics - Trento, Italy*

($^{17}$)  *Istituto Nazionale di Fisica Nucleare (INFN), Sezione di Torino - Torino, Italy*
($^{18}$)  *University of Piemonte Orientale, Department of Science and Technological Innovation - Alessandria, Italy*
($^{19}$)  *University of Napoli, Department of Physics "E. Pancini" - Napoli, Italy*
($^{20}$)  *University of Bologna, Department of Physics and Astronomy - Bologna, Italy*
($^{21}$)  *Museo Storico della Fisica e Centro Studi e Ricerche Enrico Fermi - Rome, Italy*
($^{22}$)  *University of Rome La Sapienza, Department of Scienze di Base e Applicate per l'Ingegneria (SBAI) - Rome, Italy*
($^{23}$)  *University of Milano, Department of Physics - Milano, Italy*
($^{24}$)  *University of Perugia, Department of Physics and Geology - Perugia, Italy*
($^{25}$)  *University of Perugia, Department of Engineering - Perugia, Italy*
($^{26}$)  *University of Rome La Sapienza, Department of Physics - Rome, Italy*
($^{27}$)  *Istituto Nazionale di Fisica Nucleare (INFN), Sezione di Roma Tor Vergata - Rome, Italy*
($^{28}$)  *University of Torino, Department of Physics - Torino, Italy*
($^{29}$)  *Istituto Nazionale di Fisica Nucleare (INFN), Sezione di Bari - Bari, Italy*
($^{30}$)  *CEADEN, Centro de Aplicaciones Tecnologicas y Desarrollo Nuclear - Havana, Cuba*
($^{31}$)  *Gran Sasso Science Institute - L'Aquila, Italy*
($^{32}$)  *Technische Universität Darmstadt Institut für Festkörperphysik - Darmstadt, Germany*
($^{33}$)  *National University of Science and Technology, MISIS - RUS-119049 Moscow, Russia*
($^{34}$)  *Lebedev Physical Institute of the Russian Academy of Sciences - RUS-119991 Moscow, Russia*

**Summary.** — The FOOT (FragmentatiOn Of Target) experiment aims to determine the fragmentation cross-sections of nuclei of interest for particle therapy and radioprotection in space. The apparatus is composed of several detectors that allow fragment identification in terms of charge, mass, energy and direction. The fragment time of flight (ToF) along a lever arm of $\sim$2 m is used for particle ID, requiring a resolution below 100 ps to achieve a sufficient resolution in the fragment atomic mass identification. The timing performance of the ToF system evaluated with $^{12}$C and $^{16}$O beams is reviewed in this contribution.

## 1. – Introduction

Nuclear fragmentation reactions in the energy range between $100 \, \text{MeV}/u$ and $700 \, \text{MeV}/u$ play a fundamental role both in Particle Therapy (PT) and for Radioprotection in Space (RS) applications [1]. In PT fragments are produced in the collision between therapeutical ions (typically delivered with a kinetic energy between $100 \, \text{MeV}/u$ and $400 \, \text{MeV}/u$ for $^{12}$C ions) and patient nuclei, causing the fragmentation of one (or both) of the involved nuclei. The dose released by such secondary particles has to be taken into account when planning the therapy, since it may affect the Tumor Control Probability (TCP) and the Normal Tissue Control Probability (NTCP) [2]. The same processes are of interest for RS: the Galactic Cosmic Radiation (GCR), mainly composed by protons and He ions with an average kinetic energy of $700$–$1000 \, \text{MeV}/u$, would be the

main source of dose for astronauts involved in long-term missions in deep space. To prevent serious health risks for the crew, an efficient spacecraft shielding is mandatory. Therefore, a detailed knowledge of the fragmentation reactions is required for an optimal passive shielding of spacecrafts. At present, the models implemented in the Monte Carlo simulation algorithms in the energy range of interest for such applications are not reliable, and experimental data are scarce [3,4].

The FOOT (FragmentatiOn Of Target) experiment of INFN (Istituto Nazionale di Fisica Nucleare, Italy) aims to measure the double differential cross-sections for fragmentation reactions involving proton (target fragmentation) and C, He, O (projectile fragmentation) beams at different energies. The measurement strategy is to shoot beams of C, He, O on graphite and polyethylene targets, using an inverse kinematic approach when measuring the target fragmentation induced by protons. The inverse kinematic approach is needed as the target fragments produced by proton beams would have too short ranges in matter (tens of microns) preventing the possibility of a direct measurement. The experimental apparatus (described in [5]) is optimised for the $Z \geq 3$ fragment detection and will allow for a full fragment identification in terms of charge ($Z$), mass ($A$), energy and direction. In particular, the fragment $Z$ and $A$ reconstruction will be performed exploiting their time of flight (ToF) on a $\sim 2$ m flight distance. In order to be able to identify the heaviest fragments, a ToF resolution below 100 ps is required. In this contribution the timing performance of the ToF system measured at CNAO (Centro Nazionale di Adroterapia Oncologica, Pavia, Italy), and at GSI (Darmstadt, Germany) will be reported.

## 2. – The FOOT ToF system

The ToF is measured in FOOT using two timestamping stations, both built by plastic scintillators coupled to Silicon Photomultipliers (SiPM). The former, named Start Counter (SC), is placed before the target to count the incoming ions, and provides the *start time*. The latter, named $\Delta E$-ToF, is used to evaluate the fragment $dE/dx$ and to assess the *stop time*.

**2**˙1. *Start counter*. – The SC layout consists of a homogeneous layer of EJ-228 $5 \times 5 \times 0.025$ cm$^3$, as a result of an optimisation aiming to balance the detector time resolution and the amount of material, hence to minimize the fragmentation probability before the target. The scintillator is held by an aluminum frame, enclosed in a light-tight box (shown in fig. 1) having an entrance window of aluminum Mylar ($10\,\mu$m thick). The light produced by the particles is read out by 8 groups of 6 SiPMs ASD-NUV3S (active area $3 \times 3$ mm$^2$ each) connected in series that are coupled to the scintillator side by means of a thin coat of optical grease, covering more than 70% of the perimeter.

**2**˙2. *$\Delta E$-ToF*. – The detector, already described in [6], consists of a matrix of EJ-212 bars (3 mm thick, wrapped with and ESR specular reflector) orthogonally arranged in two subsequent layers (see fig. 2). Each layer is composed of 20 bars that are 2 cm wide and 44 cm long, resulting into a $40 \times 40$ cm$^2$ active area. The light produced in each bar is collected at both the extremities using to 4 SiPMs per side (MPPC S13360-3025PE by Hamamatsu, $3 \times 3$ mm$^2$ active area) biased and read-out by a single electronic channel.

The two detectors share the SiPM read-out system: the 88 output signals of the $\Delta E$-ToF and the SC are digitized and recorded by using the WaveDAQ system [7], capable of a 0.5–5 GS/s sampling speeds, implemented using DRS4 chips [8].
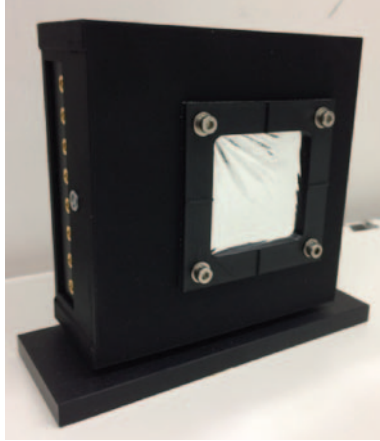
Fig. 1. – Picture of the SC box. The incoming ions are shot in the centre of the aluminum Mylar window.

## 3. – Tests with $^{12}$C and $^{16}$O beams and results

The time resolution of the apparatus has been evaluated using $^{12}$C ion beams of the CNAO therapy center at $115 \, \text{MeV}/u$, $260 \, \text{MeV}/u$ and $400 \, \text{MeV}/u$, and the $^{16}$O beam of the GSI facility with kinetic energy of $400 \, \text{MeV}/u$. The detectors have been placed at distances of $\sim 50 \, \text{cm}$ and $\sim 200 \, \text{cm}$, respectively, at CNAO and at GSI as sketched in fig. 3 (left). The beam was shot with a $1$–$10 \, \text{kHz}$ rate, as planned in the final FOOT data-taking conditions. All the bars of the $\Delta E$-ToF have been tested moving the detector by means of a step-motor following a cross centred in the detector plane, in such a way to hit each bar in its centre as shown in fig. 3 (right). Signals have been sampled at $4 \, \text{GS/s}$, recording 1024 samplings per waveform. The input signal dynamic range was $1 \, \text{V}$. An example of the signals generated by the SC and the $\Delta E$-ToF is shown in fig. 4.

**3**˙1. *Timestamp evaluation.* – The start and stop time evaluation has been performed applying a digital Constant Fraction Discriminator (dCFD) algorithm to the wave-forms, that mimics an analog CFD behaviour and reduces the impact of the amplitude
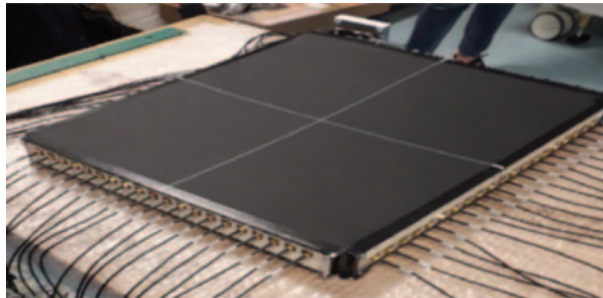


Fig. 2. – Picture of the $\Delta E$-ToF detector. The scintillator planes are enclosed in a black plastic cover that prevents the passage of light. The read-out channels, placed at the end of each bar, can be viewed.
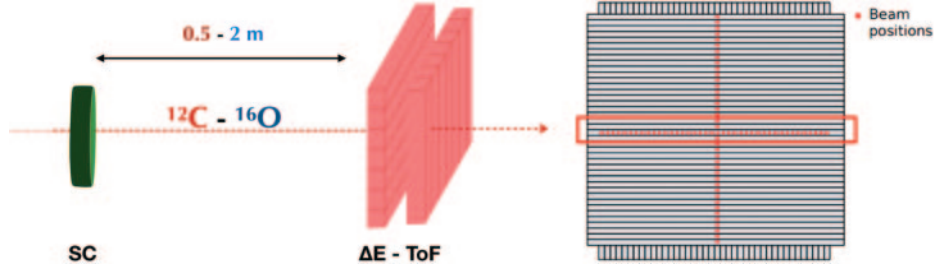
Fig. 3. – Sketch of the setup used at CNAO and GSI facilities to test the ToF system (left). Scheme of the detector irradiation (right).

fluctuations. The data proceeds as follows: each signal is delayed, amplified and inverted at first, then is added to the original signal to generate a bipolar signal, as shown in fig. 5. Finally, the zero-crossing point is taken as timestamp for each signal using a linear interpolation between the two samplings closest to the baseline having amplitudes with opposite sign. An amplitude fraction of 20% and delays of 2.0 ns and 10 ns, respectively, for the SC and the $\Delta E$-ToF signals have been used as a result of the ToF resolution minimization. The 8 SC signals have been summed up for each event, and the resulting signal has been processed according to the above-mentioned flow, taking the zero-crossing time as *start time* ($t_{\text{start}}$). The *stop time* ($t_{\text{stop}}$) is defined for each bar of the $\Delta E$-ToF detector as the arithmetic average between the signals collected at both extremities of that bar.

The phase jitter of the sampling clock caused by the routing in the different boards of the WaveDAQ system is evaluated by acquiring the clock waveforms themselves in each event. The uncalibrated ToF, not including cable differences, has been evaluated subtracting the jitter event by event.

**3**˙2. *Results*. – The ToF resolution for each bar has been evaluated as the $\sigma$ of a Gaussian fit to the ToF distribution. Due to the negligible fragmentation expected in
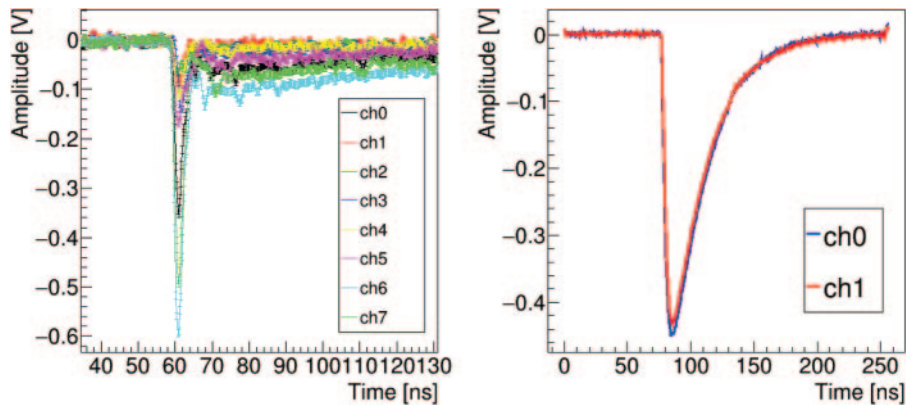


Fig. 4. – Example of the output signals of the SC (left), and of a single bar $\Delta E$-ToF (right), obtained with $^{12}$C ion beam at 260 MeV/$u$. The two shown channels (ch0 and ch1) are collected at the two opposite extremities of the same bar.
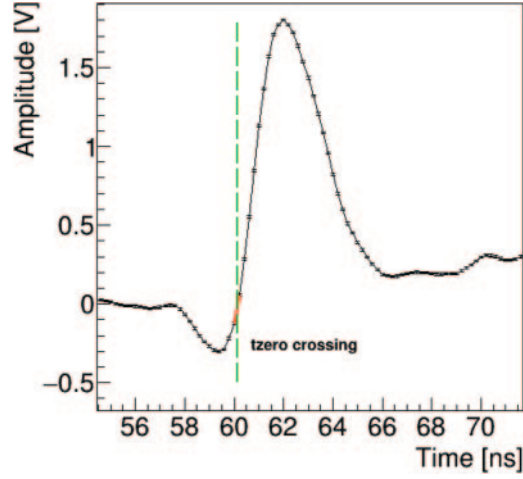
Fig. 5. – Example of a bipolar signal derived using the dCFD algorithm for the SC waveform processing.

the SC, no selection on the $\Delta E$-ToF signals has been applied. The average resolution $\sigma_{\text{ToF}}$ ranges between 55 ps and 80 ps as a function of the beam kinetic energy, as reported in fig. 6. The contribution of the $\Delta E$-ToF detector ($\sigma_{\Delta E\text{-ToF}}$) has been estimated using the time information from the horizontal and vertical bars, varying between 30 and 35 ps. As a consequence, a SC time resolution $\sigma_{\text{SC}}$ between 50 and 70 ps has been obtained according the equation $\sigma_{\text{SC}} = \sqrt{\sigma_{\text{ToF}}^2 - \sigma_{\Delta E\text{-ToF}}^2}$. As expected due to its small thickness, the SC one represents the dominant contribution to the ToF resolution.
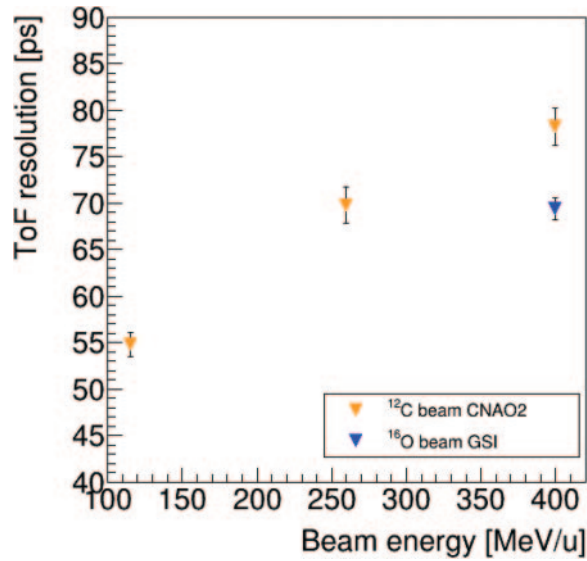


Fig. 6. – Measured ToF resolution as a function of the $^{12}$C and $^{16}$O beam energy.

### 4. – Conclusions

The FOOT ToF system has been tested with $^{12}$C and $^{16}$O ion beams with energies of interest for PT and RS applications (115 MeV/$u$–400 MeV/$u$). The measured ToF resolution matches the expectations and fulfill the requirements needed for the fragment atomic mass discrimination level needed by the cross section measurement program of the FOOT experiment.

REFERENCES

[1] ZEITLIN CARY and LA TESSA CHIARA, *Front. Oncol.*, **6** (2016) 65.
[2] TOMMASINO F. and DURANTE M., *Cancers*, **7** (2015) 1.
[3] NORBURY J. W., MILLER J., ADAMCZYK A. M. *et al.*, *Radiat. Meas.*, **47** (2012) 5.
[4] DUDOUET J. *et al.*, *Phys. Rev. C*, **89** (2014) 054616.
[5] PATERA V. *et al.*, *PoS*, **INPC2016** (2017) 128.
[6] MORROCCHI M. *et al.*, *Nucl. Instrum. Methods A*, **916** (2019) 116.
[7] GALLI L. *et al.*, *Nucl. Instrum. Methods A*, **936** (2019) 399.
[8] RITT S., *Nucl. Instrum. Methods A*, **518** (2004) 1.